NASA Technical Memorandum 79235

THE ALKALINE ZINC ELECTRODE AS
A MIXED POTENTIAL SYSTEM

William L. Fielder
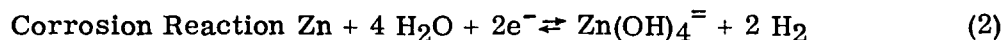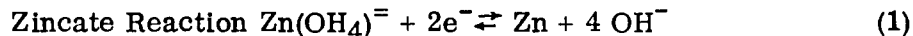Lewis Research Center
Cleveland, Ohio

July 1979

SUMMARY

The objective of this investigation on alkaline zinc electrodes was to determine the relative importance of two electrochemical processes termed the zincate and the corrosion reaction. These may occur simultaneously as a result of a mixed potential, particularly for the dilute zincate ($Zn(OH)_4^=$) concentration region – the state of the alkaline zinc battery near the end of the charging cycle. Unique ways of interpreting the mixed potential data were explored.

For this study, triangular wave and direct current pulses were supplied through a potentiostat to a zinc (Zn) rotating disk electrode (electrolyte of 0.01 molar $Zn(OH)_4^=$ and 9 molar OH^-) to investigate the cathodic and anodic processes. Diffusion calculations (via the Levich and similar equations) showed that the relative proportions of the zincate and corrosion reactions varied with potential. For the cathodic region at higher potentials, the cathodic corrosion process predominates. At a lower potential of 50 mV, the cathodic zincate and corrosion processes occur simultaneously (at a ratio of about 3:2, respectively) with the $Zn(OH)_4^=$ as the rate-controlling diffusing species. For the anodic region, at higher potentials, the anodic zincate process is the dominant one with hydroxide ion (OH^-) as the rate-controlling diffusing species. At a lower potential of 50 mV, if H_2 is present, the anodic corrosion process predominates with $Zn(OH)_4^=$ as the rate-controlling diffusing species.

INTRODUCTION

The electrochemistry of aklaline zinc (Zn)-zincate ($Zn(OH)_4^=$) systems are of considerable interest because of the desirability of using Zn electrodes for high energy density battery systems. For these Zn battery systems, three problem areas are of continuing importance: maintaining high current densities, increasing the charge-discharge cycle life, and minimizing the amount of hydrogen (H_2) evolution near the end of the charge cycle.

Bockris has suggested one explanation for the production of H_2 (ref. 1). He indicated that the rest potential for Zn in alkaline solutions is a mixed potential resulting from a $Zn(OH)_4^=$-Zn couple and a Zn-H_2 couple. Respectively, these electrode reactions are:

$$\text{Zincate Reaction } Zn(OH_4)^= + 2e^- \rightleftarrows Zn + 4\ OH^- \tag{1}$$

$$\text{Corrosion Reaction } Zn + 4\ H_2O + 2e^- \rightleftarrows Zn(OH)_4^= + 2\ H_2 \tag{2}$$

For electrolytes of moderate $Zn(OH)_4^=$ concentration, this corrosion reaction is generally considered to be relatively unimportant. However, at a lower $Zn(OH)_4^=$ concentration region, the state of the alkaline Zn battery near the end of the charging cycle, the corrosion reaction may become increasingly important.

E-141

The primary objective of the present investigation was to determine the importance of the corrosion reaction (producing H_2), relative to the zincate reaction at low $Zn(OH)_4^=$ concentrations. This was done by studying the mass transport of the rate-controlling diffusing species. Because the other two problem areas (i.e., high current densities and cycle life) are also related to the mass transport of the species, the results should contribute to the understanding of these two areas as well.

In our investigation, high purity Zn electrodes were used without any additional pretreatments to influence the corrosion reaction. The study was performed both cathodically and anodically by the application of triangular wave and direct current pulses to a Zn rotating disk electrode which served as the working electrode. The electrolye was a dilute $Zn(OH)_4^=$ solution (0.01 molar) containing 9 molar hydroxide ion (OH^-). Mass transport control was examined for both the cathodic and anodic processes under these mixed potential conditions.

All of our current-voltage data were obtained under diffusion controlled conditions as will be shown from the experimental data. Via the Levich and similar equations, diffusion coefficients and valence changes were calculated. The results of these calculations has allowed us to deduce the nature of the electrode processes in various voltage regions, both cathodic and anodic.

EXPERIMENTAL DETAILS

A schematic of the 3-electrode cell is shown in figure 1. The working electrode (A) was a rotating disk consisting of a Zn rod sealed in teflon (B). The starting material was a rod of Zn of 99.999 percent purity. It was melted at about 450° C under vacuum in a quartz tube to eliminate voids. After cooling, it was machined, degreased, and sealed into the teflon holder. The Zn working electrode (0.5 cm^2) was polished just before use with 600, 0.3 and 0.05 micrometer alumina, and then mounted for rotation. A Zn foil, of 99.999 percent purity (about 20 cm^2) was used for the counter electrode (C). A Zn wire (about 0.1 cm OD) was placed close (about 0.1 to 0.2 cm) to the working electrode. This wire, which was in contact with the aqueous zincate electrolyte (D), served as the reference electrode (E).

The electrolyte solution was 0.01 molar in potassium zincate $(K_2Zn(OH)_4)$ and 9 molar in potassium hydroxide (KOH). This solution was prepared by dissolving ZnO in aqueous KOH solution. Certified reagent grades of ZnO and 45.9 percent KOH (carbonate free) were used. For most of the experiments, argon gas (F) was bubbled slowly through the electrolyte solution before and during the experiments.

Two types of experiments were performed - both with and without rotation of the disk electrode. First, cyclic voltammograms were obtained over various potential ranges and sweep rates. For these curves, a triangular wave signal was supplied through a potentiostat. For the other type of experiment, the currents were obtained up to intervals of 1500 seconds by supplying a constant direct current potential (i.e., 50 mV cathodic or anodic) through the potentiostat. The resulting

currents for both types of experiments were determined by measuring the potential drop across a standard resistor and by recording these by means of an X-Y recorder. The rotational speeds for the working electrode were determined by means of an electronic counter.

RESULTS AND DISCUSSION

Figure 2 shows a cyclic voltammogram of the alkaline zinc electrode. It displays a single sweep (at zero rotation) which was obtained at a moderate sweep rate of 0.05 volts/second. The sweep was initiated at about 270 mV anodically and continued to about 270 mV cathodically, relative to the Zn reference electrode. As seen in figure 2, mass transport controlled regions are observed giving a cathodic peak current and an anodic limiting current. The height of the cathodic peak current is at least partially dependent on the initial anodic starting potential: for example, in figure 3, where the sweep was initiated at about zero potential, the cathodic peak current was decreased considerably.

Cathodic Processes

For most cathodic processes involving the Zn electrode operating under Tafel conditions, particularly for the more concentrated $Zn(OH)_4^=$ solutions, the cathodic corrosion reaction (eq. (2)) has been considered to be relatively unimportant (ref. 1). Thus, the rest potential of Zn has been assumed to be essentially that of the cathodic zincate reaction (eq. (1)). For mass transport conditions, however, particularly for dilute $Zn(OH)_4^=$ solutions, the relative proportions of these two reactions may vary as will be shown. In figure 3, for the initial portion of the sweep, our observed currents were much smaller initially than those which should occur in the Tafel region (activation region) (ref. 1) for the cathodic zincate reaction (dashed line) thereby indicating mass transport control. At higher potentials starting at about 300 mV, the cathodic corrosion reaction becomes increasingly more dominant as indicated by the gas evolution (undoubtedly H_2).

An effect of rotating the Zn working electrode is shown in figure 4. A reasonably large cathodic peak current was obtained at zero rotation. However, at only about 4 rotations/second (RPS), the cathodic peak current decreased considerably. Presumably, at zero rotation, an excess of the anodic products (produced during the previous anodic sweep) still remained close to the surface. This allowed the cathodic process, which uses these anodic products as its reactants, to proceed for a longer time interval before depletion occurs. After depletion, diffusion of the reactants to the surface occurred with a subsequent decrease in current. At the higher rotational speeds, these anodic products may be swept from the surface more rapidly resulting in a shorter time interval before depletion occurs. This is illustrated more clearly in another way in figure 5. The three cathodic sweeps, all at the same sweep rate, had different anodic starting potentials. The cathodic peak currents were larger for the more anodic starting points.
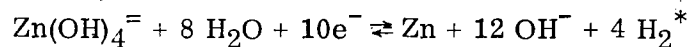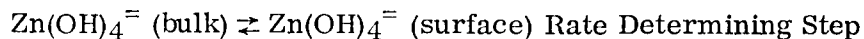
The peak current for the cyclic sweep is related to the diffusion coefficient by the Randles-Sevick equation (ref. 5). The calculations are given in appendix A, part I. For curve 3 in figure 5, all of the factors in the Randles-Sevick equation are known if the mass transport is controlled by the diffusion of $Zn(OH)_4^=$. By assuming the $Zn(OH)_4^=$ diffusion coefficient, D_o, to be the unknown, it was calculated to be about 6×10^{-5} cm^2/sec. This value is about an order of magnitude larger than the reported values: May and Kautz (ref. 2) gave a value of about 4×10^{-6} cm^2/sec; while Moshtev (ref. 4), using the rotating disk technique, gave a value of 3.5×10^{-6} cm^2/sec.

For another approach, we used cathodic direct current pulses of 50 mV. Two results, one for zero rotation of the working electrode, and one with moderate rotation, are shown in figure 6 as illustrations. At zero rotation, the current decreased rapidly with time and approached a limiting current of about 0.7 mA after about 100 seconds. A gas (assumed to be H_2) was produced at the working electrode during this pulse. The currents for zero RPS were replotted in figure 7 as suggested by the equation (appendix A, part II) relating the instantaneous currents with the diffusion coefficient under linear diffusion conditions (ref. 6). The data could be fitted to one straight line for most of the time intervals studied. The calculations are given in appendix A, part II. Once again, assuming diffusion of $Zn(OH)_4^=$, leads to a value for D_o (10^{-4} cm^2/sec) that far exceeds the reported values.

Rotating the working electrode increased the cathodic limiting currents as illustrated in figure 6. Such limiting currents were replotted in figure 8 against the square root of the angular velocity as suggested by the Levich equation (ref. 7). The data could be fitted to one straight line indicating that these cathodic processes at 50 mV were mass transport controlled. The equations and calculations for D_o, assuming $Zn(OH)_4^=$ as the rate-controlling diffusing species for the cathodic zincate process, are given in appendix A, part III a and b. For this process, the number of electrons transferred, n, is equal to 2 as required by equation (1). However, once again, the calculated value for D_o was still about an order of magnitude larger than the reported values: a D_o value of about 3×10^{-5} cm^2/sec was obtained.

It is still reasonable to assume that $Zn(OH)_4^=$ is the primary diffusing species with a D_o value of about 3.5×10^{-6} cm^2/sec. One possible explanation for this apparent discrepancy in values for D_o is that the electron transfer process involves more than 2 electrons; that is, n is larger than 2. As shown in appendix B, the limiting currents and assumed D_o lead to a value of about 9 for n. One possible explanation for this rather large value for n is that the process must be treated as one of mixed potential with both cathodic processes occurring simultaneously at 50 mV. It should be noted that these two reactions are unusual in that one of the products of the zincate reaction (Zn) can serve as one of the reactants for the corrosion reaction. Thus, if both reactions occur simultaneously, more than 2 electrons may be necessary for the overall reduction of 1 $Zn(OH)_4^=$ to Zn. For example, if about 2/3 of all the Zn (produced by the zincate reaction) reacts to produce the starting material $Zn(OH)_4^=$ (by the corrosion reaction), the overall reduction of

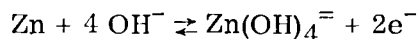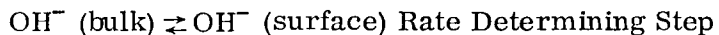each $Zn(OH)_4^=$ to Zn may require about 10 electrons. Therefore, it is proposed that the cathodic processes at 50 mV is represented as follows:

$$Zn(OH)_4^= \text{ (bulk)} \rightleftarrows Zn(OH)_4^= \text{ (surface) Rate Determining Step}$$

$$Zn(OH)_4^= + 8 H_2O + 10e^- \rightleftarrows Zn + 12 OH^- + 4 H_2{}^*$$

Presumably, the above representation will vary with cathodic potential. For example, the zincate process (relative to the corrosion process) will become more dominant at smaller potentials and less dominant at larger potentials.

Anodic Processes

The anodic corrosion reaction, particularly for the process operating at Tafel conditions, has also been considered to be unimportant relative to the anodic zincate reaction (ref. 1). However, for mass transport conditions, both anodic reactions may occur simultaneously and the proportion of these two reactions may vary with potential. (Note that dissolved H_2 must be present for anodic eq. (2) to occur.) If the zincate process is the dominant one for the anodic sweep, a larger current is to be expected because OH^- should be the primary diffusing species and the OH^- concentration in the bulk is much larger than for the $Zn(OH)_4^=$. The diffusion coefficient for the OH^- is much larger than for the $Zn(OH)_4^=$, being of the order of 5×10^{-5} cm^2/sec (ref. 8). In contrast, if the dominant process were anodic corrosion with diffusion of $Zn(OH)_4^=$, the anodic sweep should give an anodic peak, similar to the cathodic peak, with smaller currents. As seen in figure 2, the anodic sweep did give a much larger saturation current than that obtained for the corresponding cathodic sweep at the same potential; a relatively large anodic limiting current of about 125 mA was obtained at an anodic potential of about 200 mV. Therefore, it is assumed that the anodic processes (for this cyclic voltammogram at 200 mV) involved the anodic zincate reaction as the dominant one with diffusion by means of the OH^- species being the rate-controlling step:

$$OH^- \text{ (bulk)} \rightleftarrows OH^- \text{ (surface) Rate Determining Step}$$

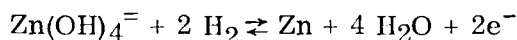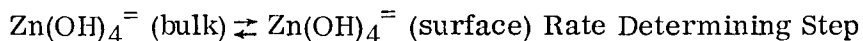$$Zn + 4 OH^- \rightleftarrows Zn(OH)_4^= + 2e^-$$

In addition, direct current pulses of 50 mV were used to investigate the anodic processes at moderately low potentials and over longer time intervals. Two results, one for zero rotation and one with moderate rotation (41 RPS) are shown in figure 9 as illustrations. At zero rotation, the current decreased rapidly with time to give a limiting current of about 2 mA; a value which is much smaller than that value of

---

*Combination of 3 equations (1) and 2 equations (2).

125 mA which was obtained for the cyclic voltammograms during the anodic sweep. Furthermore, with rotation, the current initially decreased rapidly to give a "pseudo" limiting current but then increased somewhat, after about 200 to 400 seconds, to give the final anodic limiting current. Gas evolution was not observed at the working electrode but did occur at the counter electrode. Because the counter electrode was functioning cathodically here, this was in agreement with the previous observations that a gas (i.e., H_2) was produced at the working electrode during the cathodic pulses. Moreover, this H_2, produced at the counter electrode, can migrate to the working electrode and be the starting material for reaction (2).

Both sets of anodic limiting currents were plotted in figure 10 against the square root of the angular velocity. For rotational speeds above about 7 RPS, the data for the final limiting currents could be fitted roughly to one straight line. As shown in appendix A, part III a and c, the calculated diffusion coefficient for OH^- (the assumed diffusing species for the anodic zincate reaction) is too small (i.e., of the order of 10^{-9} cm^2/sec). Therefore, in contrast to the explanation presented for the cyclic voltammogram at larger anodic potentials, the anodic zincate process with rate-controlled diffusion of OH^- is apparently not the dominant one for the final limiting current region at 50 mV. Instead, the anodic corrosion reaction is presumably of greater significance, particularly if H_2 is present at moderate concentrations. It should be noted again that H_2 was present because it was produced at the counter electrode. If one assumes that the anodic corrosion process is dominant at 50 mV, $Zn(OH)_4^=$ is expected to be the rate-controlling species for the final limiting current region (because its D_0 is about an order of magnitude smaller than that for H_2, the other reactant for the anodic corrosion reaction).[*] For example, as shown in appendix A, part III a and d, a value of about 5×10^{-6} cm^2/sec was obtained which is in reasonable agreement with the reported values for $Zn(OH)_4^=$. Therefore, it is proposed that the anodic process at 50 mV is represented in the following manner:

$$Zn(OH)_4^= \text{ (bulk)} \rightleftarrows Zn(OH)_4^= \text{ (surface) Rate Determining Step}$$

$$Zn(OH)_4^= + 2 \ H_2 \rightleftarrows Zn + 4 \ H_2O + 2e^-$$

It should be noted that the mass transport of H_2 to the electrode surface can be the rate-controlling process if the H_2 bulk concentration is sufficiently small. It is proposed that this is one possible explanation for the "pseudo" limiting current region, because initially, the concentration of H_2 in the bulk electrolyte should be small. But, as the reaction proceeds, the concentration of H_2 may increase (as suggested by the time interval of about 200 to 400 seconds to give the final limiting current). Presumably, after this time interval, the H_2 concentration has increased sufficiently to allow the diffusion of the slower species, $Zn(OH)_4^=$, to become the rate-controlling process for the final limiting current region.

---

[*]The diffusion coefficient for H_2 has been reported to be 4×10^{-5} cm^2/sec in 0.5 molar H_2SO_4 (ref. 8).

CONCLUDING REMARKS

This paper illustrates the usefulness of examining certain electrode systems as ones with mixed potentials. It also illustrates that the relative proportions of parallel processes occurring simultaneously may depend on the potential and the concentration and diffusing properties of the diffusing species. A mixed potential treatment is particularly applicable to the dilute zincate electrolyte system where the products of one reaction can serve as the reactants for the parallel reaction.

For the present investigation, triangular wave and direct current pulse methods were applied to a Zn rotating disk electrode to investigate the cathodic and anodic processes for a dilute zincate system – the state of an alkaline Zn battery near the end of the charging cycle. The data are interpreted in terms of a cell with a mixed potential; the reactions occurring could be termed as the zincate and corrosion reactions. Under the experimental conditions, it is proposed that both cathodic processes occur simultaneously at a lower potential of 50 mV at a ratio of about 3:2, respectively, with $Zn(OH)_4^=$ diffusion as the rate-controlling species. At higher cathodic potentials, the corrosion process becomes dominant. For the anodic process, it is proposed that if H_2 is present, the anodic corrosion process is dominant at a lower potential of 50 mV with $Zn(OH)_4^=$ diffusion being rate-controlling. At higher potentials, the anodic zincate process becomes dominant with OH^- diffusion as the rate-controlling species.

This interpretation is one possible explanation for the formation of H_2 during excessive charging of a pure Zn electrode; that is, H_2 can be produced even though the $Zn(OH)_4^=$ concentration has not been reduced to zero. Stopping the charging operation before the $Zn(OH)_4^=$ becomes depleted should decrease the corrosion process considerably relative to the zincate process. Furthermore, the present data also reiterates the importance of proper pretreatment of a Zn electrode for any practical alkaline Zn battery system. For example, a partial amalgamation of the Zn electrode, as commonly performed, may sufficiently displace the Zn electrode potential so that additional potential can be applied before the corrosion process becomes significant. This should allow the charging operation to proceed to a higher efficiency before the formation of any appreciable H_2.

APPENDIX A

DIFFUSION COEFFICIENT CALCULATIONS

I. Randles-Sevick Equation

a. Equation:

$$i_p = kn^{3/2} AD^{1/2} C_B V^{1/2} \text{ (ref. 6)}$$

where i_p is the peak current (mA); k is the Randles-Sevick constant; n is the number of electrons; A is the area (cm^2); D is the diffusion coefficient of the diffusing species (cm^2/sec); C_B is the bulk concentration of the diffusing species (m/1); and V is the sweep rate (V/sec).

b. Diffusion Coefficient of $Zn(OH)_4^=$, D_o, at 50 mV Cathodic: (Assuming data for curve 3, figure 5 for the cathodic zincate process.)

$$7 = (2.6 \times 10^5)(2)^{3/2} (0.5)(D_o)^{1/2} (10^{-2})(0.06)^{1/2}$$

$$D_o \simeq 6 \times 10^{-5} \text{ cm}^2/\text{sec}$$

II. Current-Time Relation at Linear Diffusion Conditions

a. Equation:

$$i_t = \frac{nFAC_B D^{1/2}}{\pi^{1/2} t^{1/2}} \text{ (ref. 6)}$$

where i_t is the instantaneous current (mA); F is the Faraday (96,500 coulombs/equivalent); and t is the time (sec).

b. Diffusion Coefficient of $Zn(OH)_4^=$, D_o, at 50 mV Cathodic: (Assuming data for figure 7 for the cathodic zincate process.)

$$(3.20 - 0.88) = \frac{(2)(9.65 \times 10^4)(0.5)(10^{-2})(D_o)^{1/2}(0.5 - 0.1)}{1.77}$$

$$D_o \simeq 10^{-4} \text{ cm}^2/\text{sec}$$

III. Levich Equation

a. Equation:

$$i_l = \frac{0.62 \, nFAC_B D^{2/3} W^{1/2}}{V^{1/6}} \quad \text{(ref. 7)}$$

where i_l is the limiting current (mA); W is the angular velocity (where $W = 2\pi$ RPS); and V is the kinetic viscosity of the electrolyte (cm^2/sec). The viscosity was experimentally determined to be 3.0×10^{-2} cm^2/sec.

b. Diffusion Coefficient of $Zn(OH)_4^=$, D_o, at 50 mV Cathodic: (Assuming data for figure 8 for the cathodic zincate process.)

$$(16.2 - 0.7) = \frac{(0.62)(2)(9.65 \times 10^4)(0.5)(10^{-2})(D_o)^{2/3}(225)^{1/2}}{(3.0 \times 10^{-2})^{1/6}}$$

$$D_o \simeq 3 \times 10^{-5} \, cm^2/sec$$

c. Diffusion Coefficient of OH^- at 40 mV Anodic: (Assuming data for figure 10 for the final limiting current region for the anodic zincate process.)

$$(5.85 - 3.25) = \frac{(0.62)(0.5)(9.65 \times 10^4)(0.5)(9)(D)^{2/3}\left[(225)^{1/2} - (56)^{1/2}\right]}{(3.0 \times 10^{-2})^{1/6}}$$

$$D \simeq 10^{-9} \, cm^2/sec$$

d. Diffusion Coefficient of $Zn(OH)_4^=$, D_o, at 50 mV Anodic: (Assuming data of figure 10 for the final limiting current region for the anodic corrosion process.)

$$(5.85 - 3.25) = \frac{(0.62)(0.5)(9.65 \times 10^4)(0.5)(10^{-2})(D_o)^{2/3}\left[(225)^{1/2} - (56)^{1/2}\right]}{(3.0 \times 10^{-2})^{1/6}}$$

$$D_o \simeq 5 \times 10^{-6} \, cm^2/sec$$

APPENDIX B

## NUMBER OF ELECTRONS TRANSFERRED

I. Levich-Equation

a. Number of Electrons Transferred, n, at 50 mV Cathodic: (Assuming data for figure 8 for diffusion of $Zn(OH)_4^=$ for the cathodic zincate and corrosion processes and assuming D_O of $Zn(OH)_4^=$ of 3.5×10^{-6} cm^2/sec (ref. 4).

$$(16.2 - 0.7) = \frac{(0.62)(n)(9.65 \times 10^4)(0.5)(10^{-2})(3.5 \times 10^{-6})^{2/3}(225)^{1/2}}{(3.0 \times 10^{-2})^{1/6}}$$

$$n \simeq 9$$

REFERENCES

1. Bockris, J. O'M.; Nagy, Z.; and Damjanovic, A.: On the Deposition and Dissolution of Zinc in Alkaline Solutions. J. Electrochem. Soc., vol. 119, no. 3, Mar. 1978, pp. 285-295.

2. May, Charles E.; and Kautz, Harold: Determination of the Zincate Diffusion Coefficient and Its Application to Alkaline Battery Problems. NASA TM-73879, 1978.

3. Kautz, Harold E.; and May, Charles E.: Decay of the Zincate Concentration Gradient at an Alkaline Zinc Cathode After Charging. NASA TM-79106, 1979.

4. Moshtev, R. V.; and Zlatilova, P.: Kinetics of Growth of Zinc Dendrite Precursors in Zincate Solutions. J. Appl. Electrochem., vol. 8, no. 3, 1978, pp. 213-222.

5. Adams, Ralph N.: Electrochemistry at Solid Electrodes. Marcel Dekker, Inc., 1969, p. 124.

6. Adams, Ralph N.: Electrochemistry at Solid Electrodes. Marcel Dekker, Inc., 1969, p. 50.

7. Adams, Ralph N.: Electrochemistry at Solid Electrodes. Marcel Dekker, Inc., 1969, p. 83.

8. Adams, Ralph N.: Electrochemistry at Solid Electrodes. Marcel Dekker, Inc., 1969, p. 221.
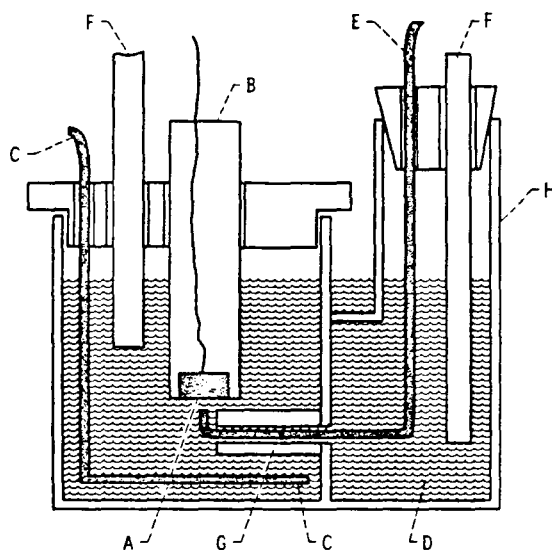
A. Zinc rod working electrode (0. 5 cm^2)

B. Teflon holder for working electrode

C. Zinc foil counter electrode

D. Zincate electrolyte solution (0. 01 molar $K_2Zn(OH)_4$ and 9 molar KOH)

E. Zinc wire reference electrode (0. 1 to 0. 2 cm from working)

F. Argon tube

G. Capillary tubing

H. Polymethylmethracrylate container
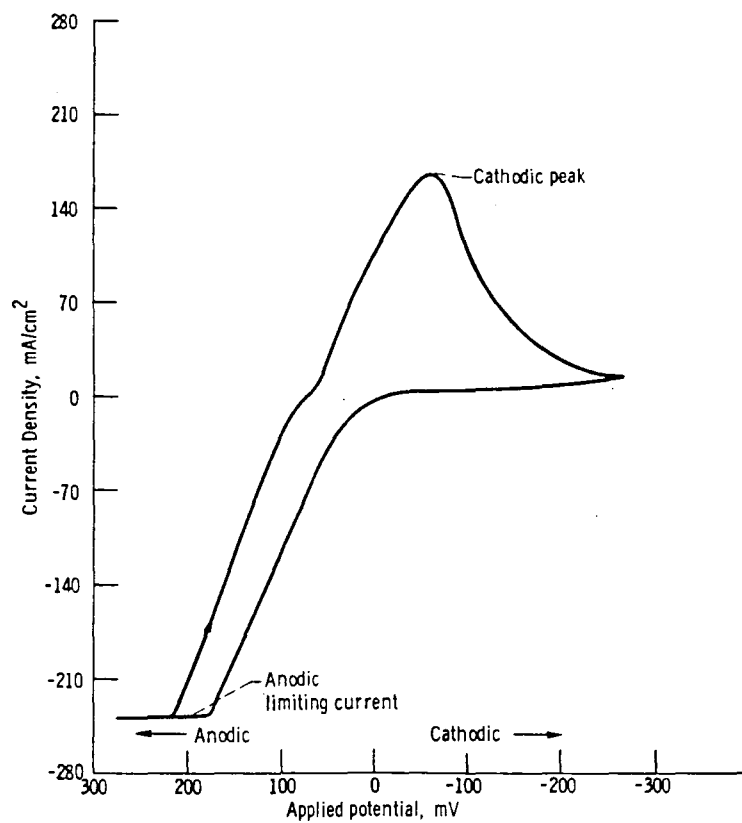
Figure 1. - Schematic of 3-electrode cell.

Figure 2. - Cyclic voltammogram obtained for zinc working electrode at zero rotation: Sweep at 0.05 V/sec starting anodically. Electrolyte of 0.01 M $Zn(OH)_4^{-2}$ and 9 M OH^-.
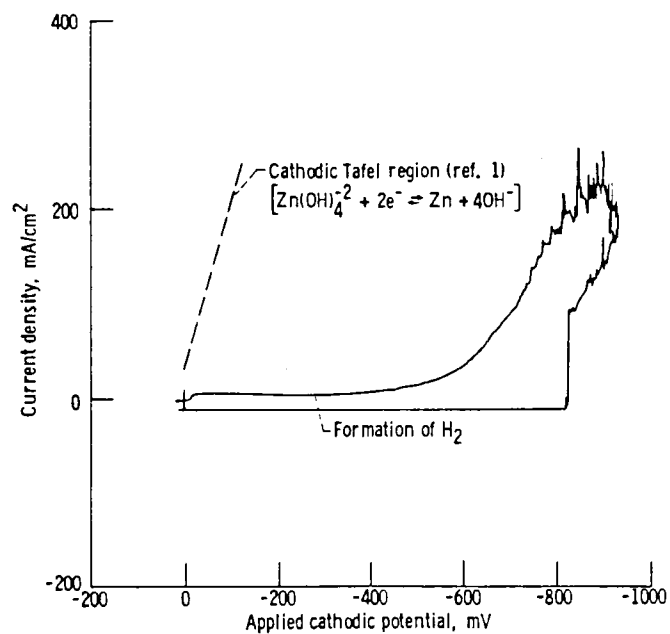
Figure 3. - Cyclic voltammogram obtained for zinc working electrode at zero rotation. Sweep at 0.1 V/sec; starting at zero potential. Electrolyte of 0.01 M $Zn(OH)_4^{-2}$ and 9 M OH^-.
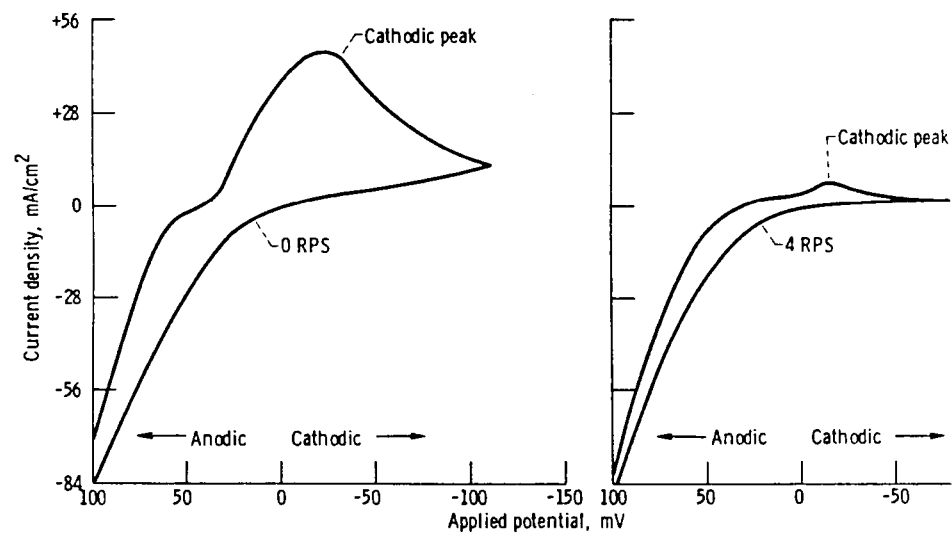
Figure 4. - Continuous cyclic voltammogram obtained for zinc working electrode for various rotational speeds. Sweep at 0.02 V/sec; starting anodically. Electrolyte of 0.01 M $Zn(OH)_4^{-2}$ and 9 M OH^-.
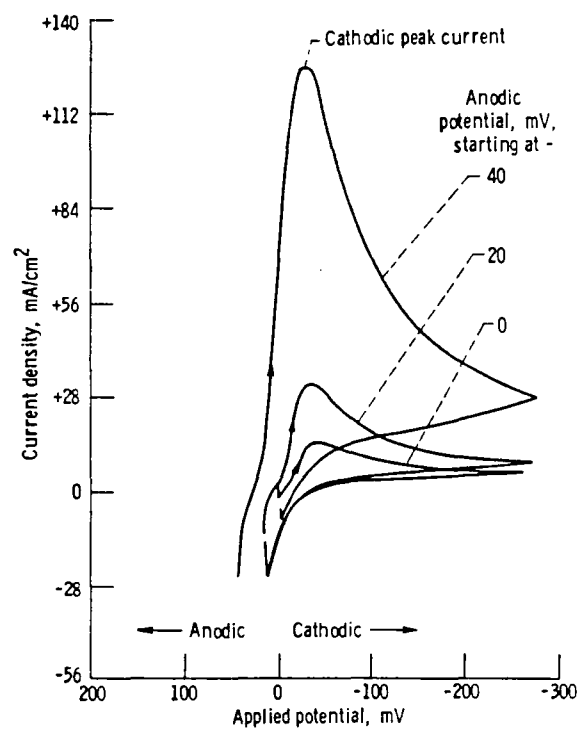
Figure 5. - Cyclic voltammogram for zinc working electrole at zero rotation. Sweep at 0.06 V/sec; starting at various anodic potentials. Electrolyte of 0.01 M $Zn(OH)_4^{-2}$ and 9 M OH^-.
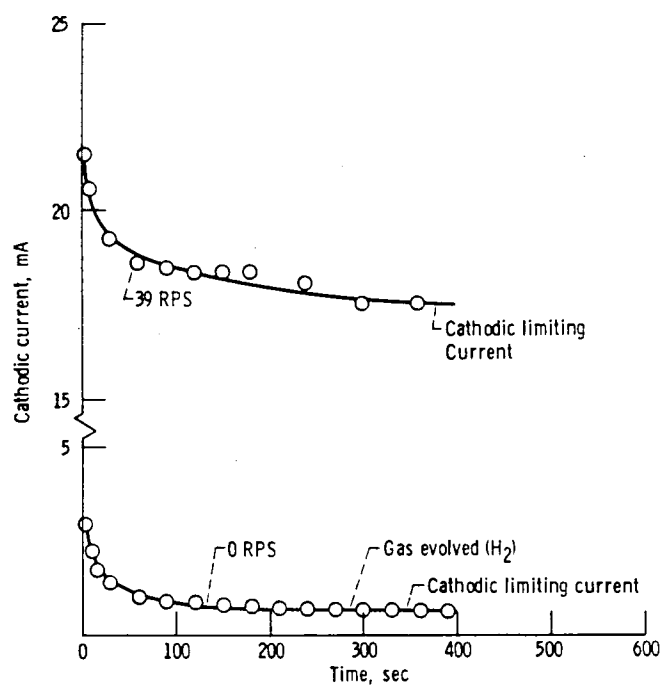
Figure 6. - Dependence of cathodic current on time for 50-mV d.c. pulse. Electrolyte of 0.01 M $Zn(OH)^{-2}$ and 9 M OH^-; working electrode area, 0.5 cm^2.
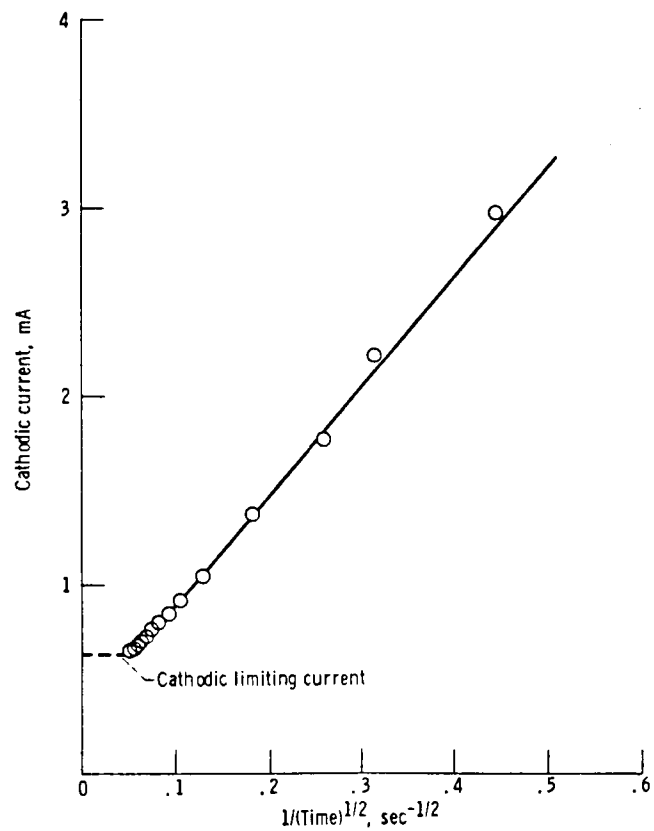
Figure 7. - Cathodic current as function of time for 50-mV d.c. pulse, at zero rotation. Electrolyte of 0.01 M $Zn(OH)_4^{-2}$ and 9 M OH^-; working electrode area, 0.5 cm^2.
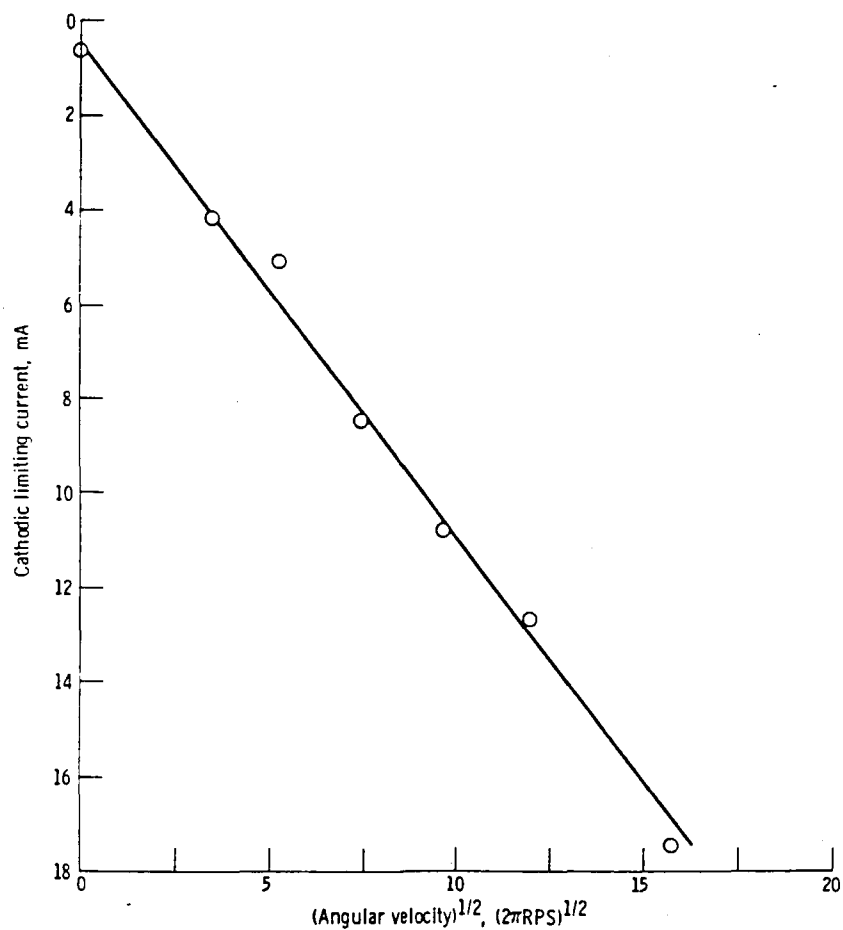
Figure 8. – Cathodic limiting currents versus angular velocity for 50-mV d.c. pulse. Electrolyte of 0.01 M $Zn(OH)_4^{-2}$ and 9 M OH^-; working electrode area, 0.5 cm^2.
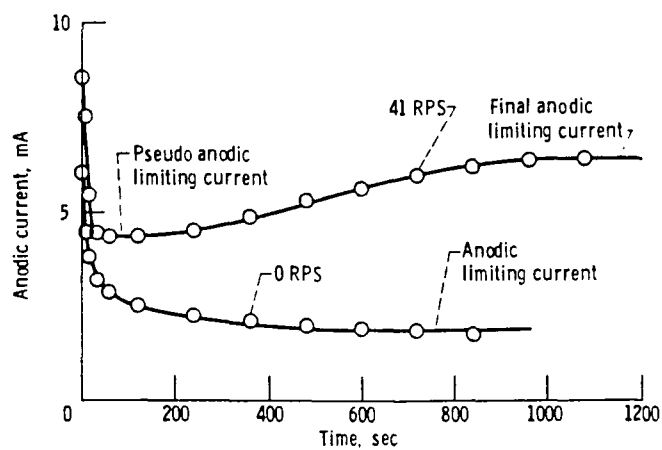
Figure 9. - Dependence of anodic current on time for 50-mV d.c. pulse Electrolyte of 0.01 M Zn(OH)$_4^{-2}$ and 9 M OH$^-$; working electrode area, 0.5 0.5 cm^2.
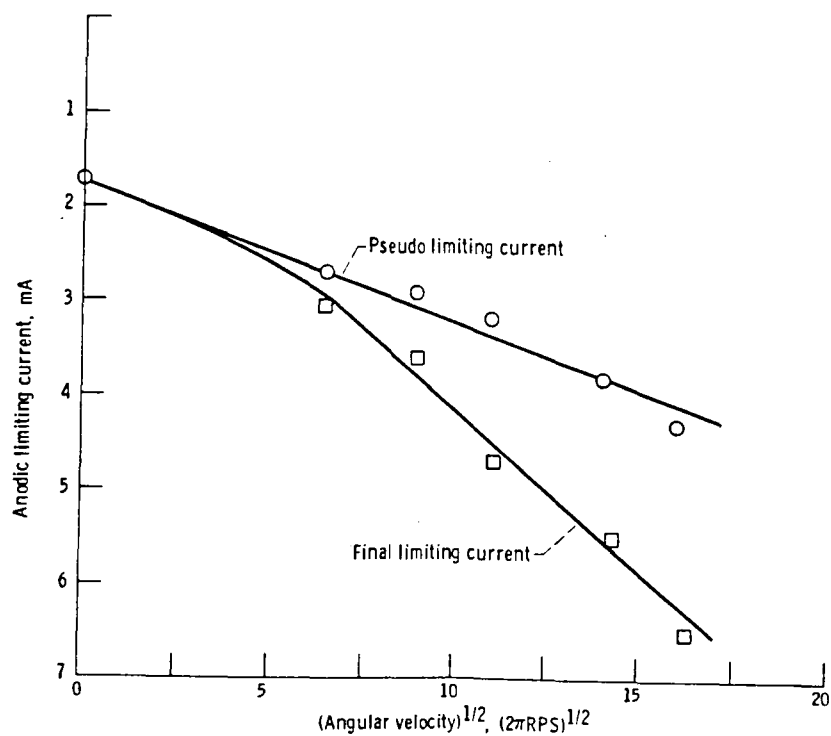

Figure 10. - Anodic limiting currents versus angular velocity for 50 mV pulse. Electrolyte of 0.01 M Zn(OH)$^{-2}$ and 9 M OH$^-$; working electrode area, 0.5 cm^2.

1. Report No. NASA TM-79235	2. Government Accession No.	3. Recipient's Catalog No.
4. Title and Subtitle THE ALKALINE ZINC ELECTRODE AS A MIXED POTENTIAL SYSTEM		5. Report Date July 1979
		6. Performing Organization Code
7. Author(s) William L. Fielder		8. Performing Organization Report No. E-141
		10. Work Unit No.
9. Performing Organization Name and Address National Aeronautics and Space Administration Lewis Research Center Cleveland, Ohio 44135		11. Contract or Grant No.
		13. Type of Report and Period Covered Technical Memorandum
12. Sponsoring Agency Name and Address National Aeronautics and Space Administration Washington, D.C. 20546		14. Sponsoring Agency Code

15. Supplementary Notes

16. Abstract

Cathodic and anodic processes for the alkaline zinc electrode in 0.01 molar zincate electrolyte (9 molar hydroxide) were investigated. Cyclic voltammograms and current-voltage curves were obtained by supplying pulses through a potentiostat to a zinc rotating disk electrode. The data are interpreted by treating the system as one with a mixed potential; the processes are termed the zincate and corrosion reactions. The relative proportions of the two processes vary with the supplied potential. For the cathodic region, the cathodic corrosion process predominates at higher potentials while both processes occur simultaneously at a lower potential (i.e., 50 mV). For the anodic region, the anodic zincate process predominates at higher potentials while the anodic corrosion process is dominant at a lower potential (i.e., 50 mV) if H_2 is present.

17. Key Words (Suggested by Author(s)) Electrochemical cells Alkaline zinc electrode	18. Distribution Statement Unclassified - unlimited STAR Category 44

19. Security Classif. (of this report) Unclassified	20. Security Classif. (of this page) Unclassified	21. No. of Pages	22. Price*

End of Document